Technical Report

Effect of the Microstructure on the Spring Properties of Stainless Steel Rods for High Performance Springs

Shota YAMASAKI* Kohji TAKANO
Masayuki TOHJO Hiroki SAKAI
Masayuki TENDO Toshihiro ISHIKAWA

Abstract

The evaluation technology of precision spring properties was developed in order to further improve the strength and elastic coefficient that contribute to the weight reduction of stainless steel springs, and stress relaxation properties that contribute to precise restoring force. The influence of microstructures on the spring properties of stainless steel wire for high-performance springs was then investigated. In the case of stainless steel springs, the combination of alloy design and manufacturing process creates characteristic materials, for example, metastable austenitic stainless steel with added C, N, which features high strength, and precipitation-hardening type metastable austenitic stainless steel with added Al, Mo, which features stress relaxation resistance, and then duplex stainless steel featuring high rigidity modulus and corrosion resistance. In addition, it is effective to optimize the manufacturing process such as the aging conditions for further improvement of the stress relaxation properties. The relationship between these steels and their manufacturing processes and microstructures such as the austenite stability and C, N, nanoclusters, and mobile dislocations was discussed.

1. Introduction

Stainless steel is produced in about 50 million tons/year worldwide and in about 3 million tons/year in Japan. Domestic stainless steel bars and wire rods account for about 300 000 tons/year, less than 10% of the total. They are used for hard drawing, cold heading, free cutting, welding, etc.[1] Stainless steel springs are classified for hard drawing applications and are mainly used as compression coil springs in a wide range of applications such as electric home appliances, automobiles, precision equipment, and medical equipment.[2]

Figure 1 shows a typical stainless steel spring manufacturing process. The rod manufacturer hot rolls stainless steel wire rods, the wire manufacturer solution heat treats and draws the wire rods into wires, and the spring manufacturer coils, solution heat treats, sets, and otherwise processes the wires into springs. The JIS G 4314[3] specifies five stainless steels for springs: SUS304, SUS302, SUS 304N1, SUS316, and SUS631J1. These steels are used in various environments according to their properties. Mechanical properties required for springs include strength, permanent set resistance (stress relaxation resistance), fatigue resistance, and modulus of elasticity.[4] The properties required of stainless steel springs are based on corrosion resistance. The main properties are the strength and modulus of elasticity that contribute to the weight reduction of the end products, and warm-temperature permanent set resistance that contributes to a precise restoring force in a warm environment. **Figure 2** schematically shows the strength and stress relaxation resistance of stainless steels for springs. The metastable austenitic stainless steel SUS304 transforms to stress-induced martensite and work hardens when

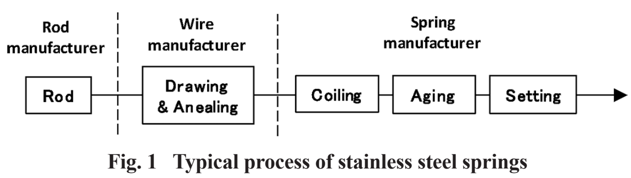

Fig. 1 Typical process of stainless steel springs

* Senior Researcher, Plate, Bar & Wire Rod Research & Development Div., Research & Development Center, Nippon Steel Stainless Steel Corporation
3434 Ooaza-shimata, Hikari City, Yamaguchi Pref. 743-8550

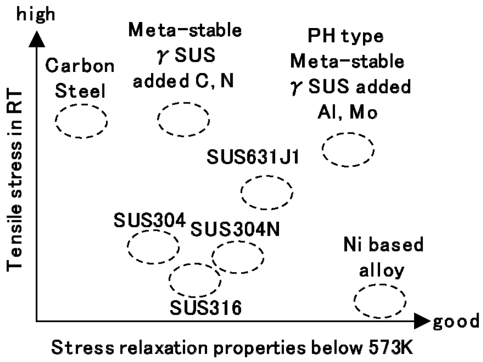

Fig. 2 Schematic map of strength and stress relaxation properties of SUS wires for spring

drawn into wires. It exhibits excellent strength and warm-temperature permanent set resistance by work hardening and is used in a wide range of applications. The SUS631J1 is classified as precipitation-hardening metastable austenitic stainless steel. Wire drawing causes its transformation to the stress-induced martensite. Aging forms the NiAl intermetallic compounds.[5] The SUS631J1 has the highest modulus of elasticity of general-purpose stainless steels for springs and exhibits excellent warm-temperature permanent set resistance. Thanks to these properties, the SUS631J1 is mainly used in springs related to automobile engines. It is not always easy for general-purpose stainless steels such as the SUS304 and the SUS631J1 to meet the increasingly severe strength, modulus of elasticity, and warm-temperature permanent set resistance requirements of springs in recent years. These mechanical properties largely depend on the microstructures (nanoclusters, mobile dislocations, etc.) controlled by a combination of the alloy compositions and manufacturing steps (wire drawing, aging, setting, etc.). These microstructure controls are considered important in improving the properties of springs. The properties of springs such as warm-temperature permanent set resistance are usually evaluated by using coil springs. We think that evaluating the precise properties of springs in the wire condition will lead to the quick proposal of appropriate spring materials and processes in various environments.

Nippon Steel Stainless Steel Corporation has been carrying out the research and development of stainless steels for high-performance springs and the proposal of solution technology by controlling microstructures through the optimization of steel composition design and manufacturing processes and by utilizing precise spring property evaluation technology. In this study, we report the effect of microstructures of these stainless steels on the properties of high-performance springs.

2. Technology for Precise Evaluation of Properties of Springs by Torsion Test

2.1 Method for evaluating warm-temperature permanent set resistance of compression coil springs

The method for evaluating the warm-temperature permanent set resistance of compression coil springs is specified by the JSMA SD010 "Compression Coil Spring Heat Resistance Test Method" of the Japan Spring Manufacturers Association.[6] A coil spring is compressed to an arbitrary height L, tightened with a jig, and held in a heat treatment furnace at a predetermined temperature T for a predetermined time t. The load loss ΔF (N) at the arbitrary height L before and after the heat treatment is measured. The permanent set resistance of the coil spring is evaluated by using the residual shear strain γ (%).

$$\gamma = \frac{\Delta\tau}{G} = \frac{8D\Delta F}{\pi D^3 G} \times 100 \qquad (1)$$

where $\Delta\tau$ is the shear stress loss (N/mm^2), D is the coil diameter (mm), d is the wire diameter (mm), and G is the modulus of rigidity (N/mm^2). This is a stress relaxation test to evaluate the stress relaxation under constant strain. It is considered that the warm-temperature permanent set resistance can be evaluated by a warm stress relaxation test. In addition, the stress in the transverse section of the wire of the compression coil spring is mainly torsion.[7] It is thus considered that the permanent set resistance of the compression coil spring can be simulated by the torsion stress relaxation test of the wire.

2.2 Outline of torsion tester for wires

The wire torsion tester can simulate the stress state of the compression coil spring by applying a torsion stress to the wire. **Figure 3** shows the appearance of the wire torsion tester.[8] The chucked wire is coupled to the tester. The wire is twisted by rotating the coupling on one side by a servo motor with an encoder. The torsion angle is output. The torque is detected at the other coupling. When the specimen is covered with a hot air basin, it can be tested warm.

The torsion tester can perform the following tests to apply the torsion stress: (1) twist test to evaluate the modulus of rigidity, twist value, torsion offset stress, torsion strength, etc.; (2) torsion stress relaxation test to evaluate torque relaxation at constant torsion angle; (3) torsion creep test to evaluate the change in the twist angle at constant torque; and (4) torsion fatigue test to evaluate the number of cycles to failure by applying torque and twist angle amplitudes at arbitrary frequency, average torque, and average twist angle.

The torsion tester has a high torque detection capability and can precisely grasp the change over time in stress relaxation and creep. The effects of wires on these properties of springs in the wire condition can also be evaluated by changing the steels and manufacturing processes described above.

2.3 Comparison of torsion stress relaxation test with conventional test

To evaluate the validity of the torsion stress relaxation resistance with the wire torsion tester, the torsion stress relaxation resistance was evaluated as compared with that determined in a conventional test.[9] A torsion stress relaxation test was conducted at room temperature to 573 K by using ϕ2.0 mm SUS304 wires aged at 673 K for 1.8 ks after drawing with an area reduction of 75%. In the torsion stress relaxation test, the relationship between the torque T (Nm) and the torsion angle θ (rad) was obtained beforehand in the torsion test at each temperature. The shear stress τ and the shear strain γ in

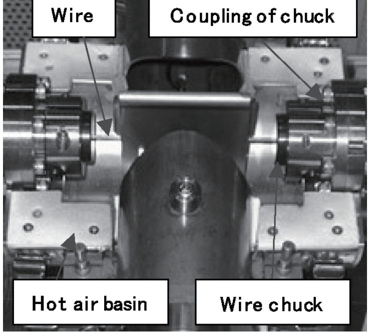

Fig. 3 Appearance of torsion tester for steel wire[8]

the outermost layer of the wire were calculated by Equations (2) and (3), respectively.[9] The shear strain γ_0 to maintain the initial shear stress τ_0 at about 600 MPa (550 to 650 MPa) was selected.

$$\tau = \frac{4\,(3T+\theta\,\frac{dT}{d\theta})}{\pi D^3} \qquad (2)$$

$$\gamma = \frac{D\theta}{2L} \qquad (3)$$

where D is the diameter of the wire drawn with an area reduction of 75% (mm) and L is the distance between the chucks (=150) (mm). In the warm test, the specimen was held at each test temperature for 3.6 ks for temperature equalization in the hot air basin and then held at the specified shear stress. The shear stress τ up to 86 ks was measured. The stress relaxation ratio (*SRR*) expressed by Equation (4) was used as an index of stress relaxation resistance.

$$SRR = (1-\frac{\tau}{\tau_0}) \times 100 \qquad (4)$$

Figure 4 shows the effect of the test temperature on the stress relaxation ratio of ϕ2.0 mm SUS304 wires drawn with an area reduction of 75% and aged at 673 K for 1.8 ks.[8] The stress relaxation ratio after aging at 298 K for 86 ks was about 0.5% and increased by increasing the test temperature. Within about 10 ks from the start of the test at each test temperature, the stress relaxation progressed to a half of that at the completion of the test. It is considered that the movement of mobile dislocations at the initial stage of the test governs the warm-temperature permanent set resistance. To compare the results of the torsion stress relaxation test with the warm-temperature permanent set resistance of the coil springs, the residual shear strain γ (%) was calculated by

$$\gamma = \frac{\Delta\tau}{G} = \frac{16\Delta T}{\pi D^3 G} \times 100 \qquad (5)$$

where G is the modulus of rigidity at each test temperature (N/mm^2) and ΔT is the torque loss (Nm).

Figure 5 shows the residual shear strain of compression coil springs in the present test and the conventional test.[8] The residual shear strain measured by the torsion stress relaxation test is almost the same as that measured in the conventional test. It is considered that the permanent set resistance of compression coil springs can be simulated by the torsion stress relaxation test of wires.

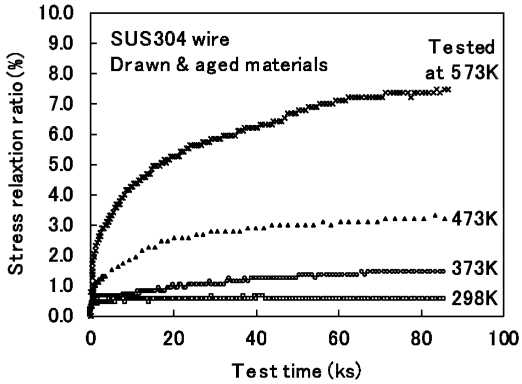

Fig. 4 Effect of test temperature on stress relaxation ratio of SUS304 steel wire (ϕ2.0 mm) aged at 673 K×1.8 ks after drawing (Red. 75%)[8]

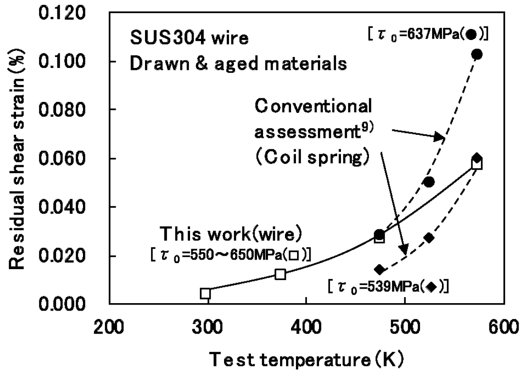

Fig. 5 Residual shear strain of torsion test and conventional coil spring test[8]

3. Factors Affecting Strength and Stress Relaxation Resistance of Stainless Steel Wires for High-Performance Springs

Table 1 shows the typical compositions of steels for high-performance springs and general-purpose steels for springs. The Md_{30} in the table is defined as the temperature at which 50% of the austenite content transforms to stress-induced martensite when a true strain of 30% is applied. It is used as an index for the mechanical stability of austenite and is uniquely calculated from the composition and the grain size v by[10]

$$Md_{30} = 551-462(C+N)-9.2Si-8.1Mn-13.7Cr -29(Ni+Cu)-18.5Mo-68N-1.42(v-8.0) \qquad (6)$$

Stainless steels for high-performance springs include C- and N-added metastable austenitic stainless steel characterized by high strength, Al- and Mo-added precipitation hardening metastable austenitic stainless steels, duplex stainless steels characterized by high modulus of rigidity and corrosion resistance, and stable austenitic stainless steels characterized by non-magnetism and hydrogen embrittlement resistance.[11] The combination of these composition designs with the optimization of production steps (like aging heat treatment and setting) is expected to improve the warm-temperature permanent set resistance, an important property for stainless steel springs.

In this chapter, we focus on the following topics: 1) effect of various manufacturing histories on the stress relaxation resistance; 2) precipitation hardening stainless steel with excellent stress relaxation resistance; 3) N-added high-strength stainless steel; and 4) duplex stainless steel with excellent modulus of rigidity. We also describe the factors that influence the strength and stress relaxation resistance of stainless steels for high-performance springs.

3.1 Effect of various manufacturing histories on stress relaxation resistance

It is important to optimize the alloy composition and manufacturing steps for the stress relaxation resistance of stainless steel wires for springs. We believe that spring utilization and fabrication technology will lead to solution proposal. Conventionally, aging heat treatment and setting treatment (application of prestrain in the deformation direction) in the room to the warm temperature range have been employed as methods for suppressing the stress relaxation of springs.[12] Few reports have been published on the effect of aging and setting on the stress relaxation of stainless steels in the warm-temperature range. We investigated this effect by using a wire twist tester and general-purpose stainless steel wires.

SUS304 wires drawn to a diameter of ϕ2.0 mm with an area reduction of 75% were aged at 673 and 773 K for 1.8 ks. The wires before and after the aging were torsion stress relaxation tested at 473 K (held at the shear strain γ of 0.9).

Table 1 Typical composition of rods for high-performance and general grade for springs

(mass%)

		C	Mn	Ni	Cr	Mo	N	Other	Md_{30} (°C)	Features
JIS G 4314	SUS304	0.07	1.2	8.5	18.1	0.2	0.04		−18	–
	SUS316	0.03	1.0	10.0	16.0	2.1	0.05		−55	
	SUS304N	0.04	1.0	8.0	19.5	0.2	0.20		−87	
	SUS302	0.11	0.8	8.0	18.1	0.2	0.06		−32	
	SUS631J1	0.08	0.8	7.6	16.4	0.1	0.02	Al:1.0	37	
Meta-stable γ SUS added C, N	Type201	0.06	4.7	4.7	16.8	0.4	0.18		17	High strength
	Type301	0.10	0.7	7.1	17.0	0.3	0.06		15	
PH type Meta-stable γ SUS added Al, Mo		0.08	0.8	7.7	13.4	2.0	0.02	Al:1.0	45	High stress relaxation resistance
Duplex type SUS	SUS821L1	0.02	3.2	2.2	20.8	0.3	0.16		26	High rigidity modulus
	SUS329J3L	0.01	1.6	6.1	22.6	3.0	0.16		−136	High corrosion resistance
Stable γ SUS added N, Mo	Type304N	0.07	1.8	9.6	18.8	0.8	0.20		−158	Non-magnetic Hydrogen-embrittle-ment-resistance
	SUS316N	0.06	1.1	10.1	17.7	2.1	0.19		−163	

Figure 6 shows the effect of the aging temperature on the stress relaxation ratio at 473 K.[8] The stress relaxation ratio of the as-drawn wire was about 13% at 86 ks, meaning that the stress relaxation was promoted. The stress relaxation ratio of the wire aged at 673 K decreased to 1/3 or less of that of the as-drawn wire. The stress relaxation of the wire aged at 773 K was further suppressed. When the specimens are aged or aged at higher temperatures, mobile dislocations are pinned or annihilated. It is considered that the stress relaxation is inhibited by the aging in this way.

To investigate the effect of the room-temperature setting stress on the stress relaxation ratio, SUS304 wires treated as described in Section 2.3 were subjected to the stress relaxation stress, 0.3% proof stress, and shear stress before and after the torsion strength by using the torsion tester. These wires were then stress relaxation tested at 473 K in the same direction as when they were set.

Figure 7 shows the effect of the room-temperature setting stress on the stress relaxation ratio of SUS304 wires.[8] The stress relaxation ratio is the smallest at the room- temperature setting stress near the 0.3% proof stress. It is considered that mobile dislocations are pinned by the setting treatment. When the room-temperature setting stress is higher than the 0.3% proof stress, the stress relaxation ratio becomes larger than that of the non-set wires. It is considered that the dislocations pinned by the aging heat treatment become mobile. Care must be taken in selecting the setting stress.

The SUS631J1 shows excellent warm-temperature permanent set resistance among the five steels specified in the JIS G 4314. Its warm-temperature permanent set resistance can be improved when the mobile dislocations and NiAl clusters are properly controlled by optimizing the aging heat treatment.

SUS631J1 wires drawn to a diameter of ϕ2.0 mm with an area reduction of 75% were aged at 753 K for 0.2 to 605 ks. The wires before and after the aging were torsion stress relaxation tested at 473 K (held at the shear strain γ of 0.8) and tensile tested. The dislocation density was quantified by X-ray diffraction line profile analysis. Using a Cu target (λ = 0.15405 nm), the full width at half maximum (FWHM) was measured from the reflections from (110), (200),

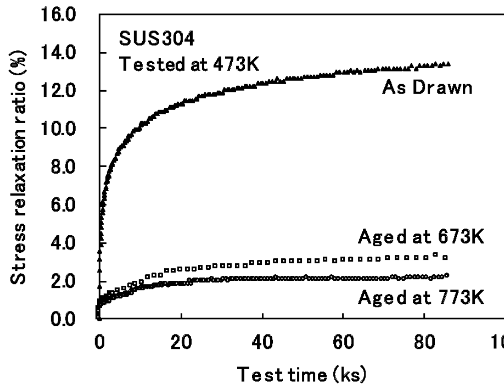

Fig. 6 Effect of aging temperatures on stress relaxation ratio at 473 K[8]

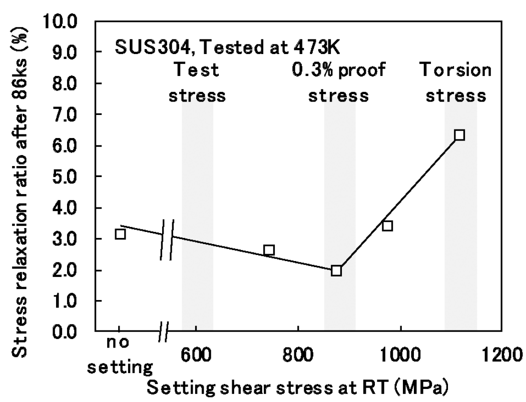

Fig. 7 Effect of setting stress at RT on stress relaxation ratio of SUS304 wire[8]

(211), (220), (310), and (222) planes. The obtained FWHM value β was substituted into the following modified Williamson-Hall[13] equation (7) and the ϕ related to microstrains like dislocations was measured.

$$\Delta K = \alpha + \phi\,(K\sqrt{C}) + O\,(K\sqrt{C})^2 \tag{7}$$

where $\Delta K = \beta \cos\theta/\lambda$, $\alpha = 0.9/D$, $K = 2\sin\theta/\lambda$, and $C = C_{h00}\,(1-qH^2)$. The Bragg reflection angle θ, crystallite size D, and C_{h00} are the constants that can be obtained from the elastic constant. The q-value is a parameter that expresses the dislocation nature. From the diffraction plane indexes, H^2 is expressed as $H^2 = \frac{(h^2k^2+k^2l^2+l^2k^2)}{(h^2+k^2+l^2)^2}$. Expansion of Equation (7) yields Equation (8). The q-value was calculated by Equation (8).

$$\frac{\Delta K^2-\alpha^2}{K^2} \approx \phi^2\, C_{h00}\,(1-qH^2) \tag{8}$$

The q-value (q_e) and the q-value (q_s) for 100% edge dislocations and 100% screw dislocations in martensitic steel are about 1.2 and 2.8, respectively.[14] The screw dislocation volume fraction S was calculated by Equation (9).

$$S = \frac{q-q_e}{q_s-q_e} \tag{9}$$

Figure 8 shows the effect of the aging time at 753 K on the stress relaxation ratio and 0.2% proof stress of the SUS631J1.[15] The 0.2% proof stress increases to about 450 MPa at 180 s, remains constant up to 18 ks, and then decreases. The stress relaxation ratio decreases with long-time aging at 753 K and becomes about 0.3% at 605 ks. The long-time aging decreases the 0.2% proof stress and suppresses the stress relaxation.

Figure 9 shows the effect of the aging time at 753 K on the ϕ-value and S-value of the SUS631J1.[15] The ϕ-value increases to 18 ks and decreases with the long-time aging. The ϕ-value is related to microstrains and is considered to arise from strains such as dislocations, solute elements, and coherent precipitates. Because the 0.2% proof stress is reduced by the long-time aging, it is considered that the decrease in the ϕ-value with the long-time aging results from the decrease in the dislocation density. The S-value is approximately 1 before and after the aging. Assuming that the microstrains measured here arise only from the dislocations, the dislocation nature of the SUS631J1 before and after the aging at 753 K is mainly considered to be spiral components. It is thought that the warm stress relaxation occurs from the cross slip of the screw dislocations. Short-time aging such as for 18 ks forms the NiAl clusters. The distance between the obstacles is shorter than before the aging. The cross slip of the screw dislocations is inhibited and thus stress relaxation is considered to be suppressed. From the X-ray profiles of specimens aged for a long time such as 605 ks, it is inferred that the decrease in the mobile dislocations with the decrease in the total dislocation density and the improvement in the pinning force of obstacles due to the ordering of NiAl clusters are factors that further suppress the stress relaxation.

3.2 Effect of NiAl and Mo-C clusters on stress relaxation resistance of precipitation hardening stainless steel wires

The SUS631J1 exhibits excellent warm-temperature permanent set resistance and high strength among the stainless steels for springs specified in the JIS G 4314. Further improvement of the warm-temperature permanent set resistance is required to contribute to a precise restoring force in a warm environment. On the other hand, there is a new precipitation hardening metastable austenitic stainless steel added with Al and Mo to render the stability of austenite lower than in the SUS631J1. The new steel is characteristic in that the austenite is transformed to the stress-induced martensite by nearly 100% by wire drawing, that fine NiAl clusters and Mo-C clusters are formed in the stress-induced martensite by the aging at high temperature, and that excellent stress relaxation resistance is

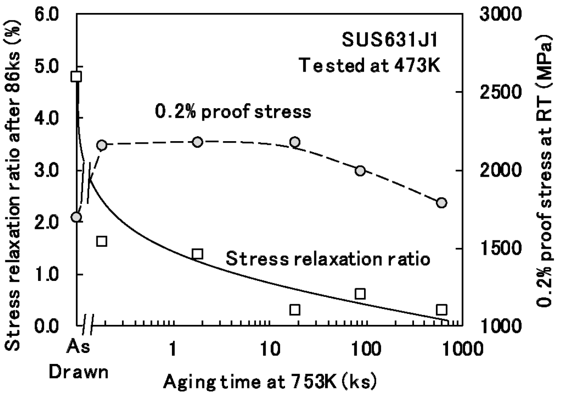

Fig. 8 Effect of aging time at 753 K on SRR and 0.2% yield stress of SUS631J1[15]

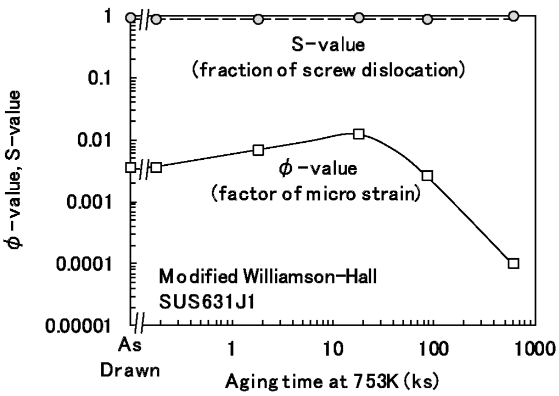

Fig. 9 Effect of aging time at 753 K on ϕ-value and S-value of SUS631J1[15]

ensured by the pinning and annihilation of mobile dislocations.

Figure 10 shows the stress relaxation behavior of various stainless steel wires aged after being drawn with an area of reduction of 75%. The aging temperature for the new steel and the SUS631J1 is 753 K. The stress relaxation ratio of the new steel is about 2% when aged at 573 K for 86 ks and is about a half of that of the SUS631J1 and about one-seventh of that of the SUS304. The new steel has excellent stress relaxation resistance. In addition, the stress relaxation ratio of the new steel at 473 K is 0.1% or less. The stress relaxation is further suppressed.

Figure 11 shows the aged tensile stress of the new steel and the SUS631J1. The age hardening amount of the new steel is about 500 MPa when aged at 753 K. Aging at higher temperatures provides the new steel with age softening resistance superior to that of the SUS631J1. For the new steel, high-temperature aging is considered to form precipitates that contribute to its precipitation hardening.

Figure 12 shows the three-dimensional atom probe (3D-AP) distribution maps of the Al for the new steel and the SUS631J1 when aged. In the 3D-AP maps, the Al and Ni are present at the same sites. The NiAl clusters with a size of several nanometers are observed. The average particle size of the NiAl clusters in the new steel is about 4.5 nm at 823 K and is smaller than 7.5 nm for the SUS631J1. This smaller particle size is considered to contribute to the improvement in the age softening resistance. Because the Mo segregation is not detected at the NiAl cluster-martensite interface, the grain refinement of the NiAl by the Mo addition is considered to

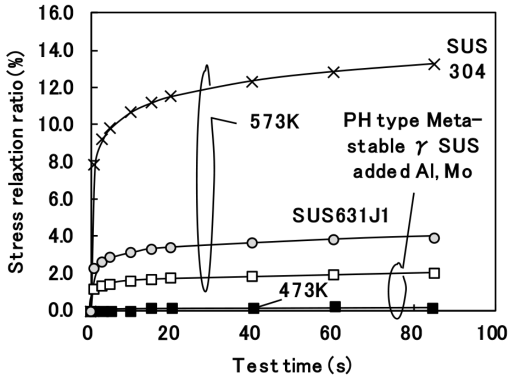

Fig. 10 Stress relaxation behavior of SUS wires aged after drawing (Red. 75%)

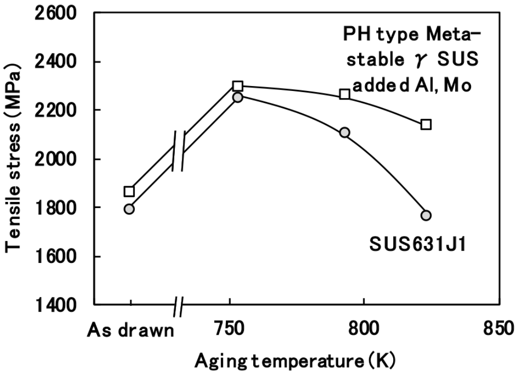

Fig. 11 Age-hardening properties of PH type Meta-stable γ SUS added Al, Mo and SUS631J1

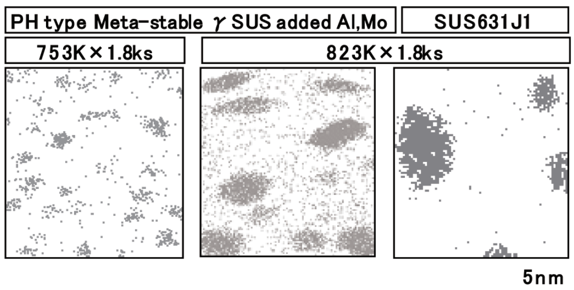

Fig. 12 Al distribution map of PH type Meta-stable γ SUS added Al, Mo and SUS631J1 (3D-AP)

inhibit the diffusion of the Al and Ni.

Figure 13 shows the carbide dispersion states examined with an extraction replica transmission electron microscope (TEM) and the 3D-AP. In the SUS631J1, coarse submicron $M_{23}C_6$ is observed. In the new steel, Mo is substituted by $M_{23}C_6$, fine carbides are formed at the martensitic lath interface, and Mo-C clusters about 2 nm in size are dispersed in the laths. As described above, it is considered that the movement of mobile dislocations in the new steel is suppressed by the grain refinement of the NiAl clusters and by the formation of the Mo-C clusters. Consequently, the new steel is considered to exhibit higher stress relaxation resistance than the SUS 631J1.

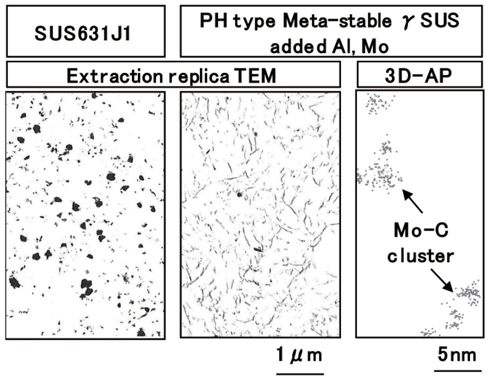

Fig. 13 Carbide dispersion state by extraction replica TEM and 3D-AP

3.3 Effect of N on strength of high-strength stainless steel wires

The metastable austenitic stainless steel SUS304 transforms to strain-induced martensite during wire drawing and shows a large work hardening. Higher strengthening is required to contribute to the weight reduction of end products. There are C- and N-added metastable austenitic stainless steels.[16, 17] These steels have the following characteristics. Decreasing the stability of the austenite promotes the stress-induced martensitic transformation during wire drawing. The strength of the stress-induced martensite is increased by the adding with C and N. The age hardening is increased by the aging heat treatment.

The ϕ2.0 mm wires of the Type 201 steel (N-added metastable austenitic stainless steel) and the SUS304 were aged at 473 to 773 K for 1.8 ks after drawing with an area reduction of 75%. Thermal analysis was performed on the specimens with a tensile tester and a differential scanning calorimetry (DSC). Fine precipitates were examined by extraction residue analysis and extraction replica TEM analysis. Nanoclusters were analyzed by the 3D-AP. The FWHM values were measured with an X-ray diffractometer (XRD).

Figure 14 shows the effect of the aging temperature on the strength of the Type 201 and SUS304 wires.[18] After 473 K aging, the tensile strength of the Type 201 is higher than that of the SUS304. The aging temperature at which the strength of the Type 201 peaks is 673 to 773 K. The secondary hardening at 673 K conventionally recognized for high-N steels is not clear.[19] The high-N Type 201 steel shows a high age hardening ability in a wide aging temperature range of 473 to 773 K. The FWHM value of the high-N Type 201 steel decreases after aging at high temperatures of 673 and 773 K. This suggests the increase in a strengthening mechanism other than dislocation strengthening.

The DSC curves of the Type 201 and SUS304 wires after wire drawing are shown in **Fig. 15**.[17] Four and three exothermic reactions are observed for the Type 201 and SUS304, respectively. The peak ① near 423 K, the peak ② near 523 K, and the peak ③ near 673 K are common to both Type 201 and SUS304. A slight exothermic reaction at the peak ④ near 773 K is observed only for the Type 201. The reaction sum of the Type 201 at 423 to 723 K is larger than that of the SUS304. The activation energy E (kJ/mol) of the exothermic reactions was calculated by Equation (10) from Kissinger plots[20] by changing the heating rate β (K/s).

$$\ln\left(\frac{T_p^2}{\beta}\right) = \frac{E}{RT_p} + \ln\frac{E}{AR} \qquad (10)$$

where T_p is the peak temperature (K), R is the gas constant, and A is a constant.

The activation energy at the peak ① (423 K) is 89 kJ/mol and is

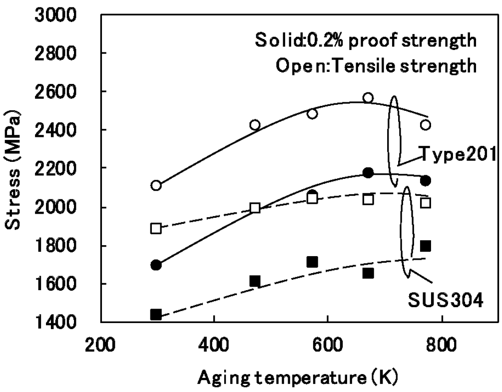

Fig. 14 Effect of aging temperature on strength of Type 201 and SUS304 steel wire[18)]

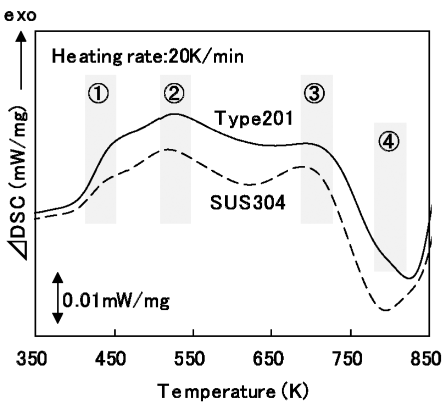

Fig. 15 DSC curves of Type 201 and SUS304 steel wire after drawing[17)]

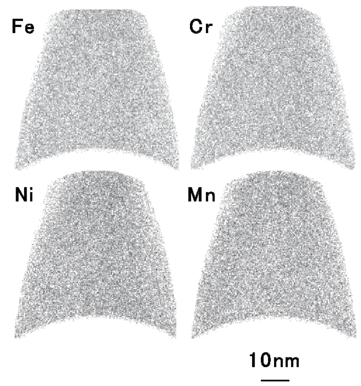

Fig. 16 Distribution map of each element of Type 201 aged at 753 K (3D-AP)[17)]

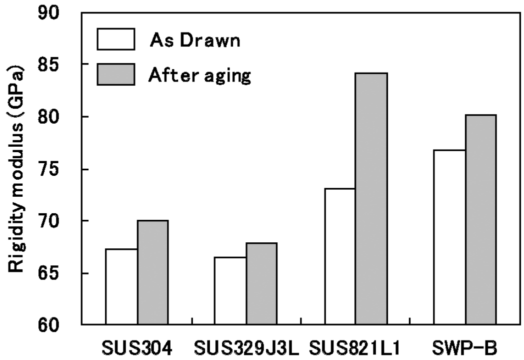

Fig. 17 Rigidity modulus of SUS wires aged after drawing (Red. 75%)[27)]

close to the activation energy of the diffusion of the C and N in α-Fe (84, 79 kJ/mol[21)]). The activation energy at the peak ② (523 K) is 147 kJ/mol and is close to the activation energy of the diffusion of the C and N in γ-Fe (148, 169 kJ/mol[21)]). The activation energy at the peak ③ (673 K) is 220 kJ/mol and is close to the activation energy of the diffusion of Cr in the SUS304 (245 kJ/mol[22)]).

From the extraction residue analysis and TEM analysis, Cr_2N precipitates about 50 nm in size were recognized in a small volume fraction of about 0.1 in the 773 K aged specimens of the Type 201, but were not recognized in the 673 K aged specimens of the Type 201. **Figure 16** shows the distribution maps (3D-AP) of the respective elements in the 753 K aged specimens of the Type 201.[17)] Although the distribution of the N overlaps the peak of Si atoms, the clustering tendency of the Cr, Ni, Fe, and Mn atoms is not observed in the 753 K aged specimens. Therefore, the main factor for the age hardening of the Type 201 at 673 K and below is presumed to be the interaction between the N and the dislocations in the stress-induced martensite and the austenite. The Cr_2N is observed in the specimens at a high temperature near 773 K, but its contribution to the strength is small. Strengthening by the interstitial-substitutional (I-S) pairs and N clusters is considered.[23, 24)]

3.4 Duplex stainless steel wires with excellent modulus of rigidity

Duplex stainless steels exhibit excellent mechanical properties, corrosion resistance, and stress corrosion cracking resistance (SCC). They are thus used in a wide range of applications.[25)] They are also used in hard-drawn wire applications such as springs and ropes. The SUS329J3L with relatively stable austenite is conventionally available as a duplex stainless steel that can be used in the hard-drawn wire applications. The SUS329J3L has excellent corrosion resistance, but its work hardening by wire drawing is smaller than for the SUS304.[26)] This restricted the design application of the SUS329J3L. In recent years, duplex stainless steels with metastable austenite have appeared and SUS821L1 is one such example. The SUS821L1 shows higher work hardening than the conventional SUS329J3L and satisfies the Class B strength requirements of stainless steel wires for springs in general-purpose applications.[26)] **Figure 17** shows the modulus of rigidity of various stainless steel wires drawn with an area reduction of 75% and aged.[27)] The modulus of rigidity of the SUS821L1 wires is about 85 GPa, is about 20% higher than 70 GPa for the SUS304, and is equivalent to or higher than that of piano wires (SWP-B). The SUS821L1 is expected to contribute to the weight reduction of stainless coil springs. There is a report that says that coil springs made of duplex stainless steels with metastable austenite exhibit stress relaxation resistance, SCC resistance, dimensional variability, and fatigue resistance equal to or higher than those of the SUS304.[28)] Further developments are expected.

4. Conclusions

To improve the strength and modulus of elasticity that contribute to the weight reduction of stainless coil springs and the warm-temperature permanent set resistance that contributes to the precise restoring force in a warm environment, we developed the technology for evaluating the precise properties of springs with a wire torsion tester and investigated the effect of the microstructures of stainless steels for high-performance springs on the properties of springs produced from them. It is possible to control microstructures as regards austenite stability, C and N utilization, nanoclusters, and mobile dislocations by the proper combination of the alloy design and manufacturing process. In this way, we can achieve high strength, stress relaxation resistance, and modulus of rigidity. In the future, unprecedented needs may appear with the structural changes in society. We will continue our relentless development activities to improve the performance of stainless steel wires for springs and other uses by controlling the microstructures according to metallurgical principles and to the findings of this study.

References

1) Hasegawa, M.: Stainless Steel Handbook. 3rd ed. Tokyo, Nikkan Kogyo Shimbun, 1995, p.676
2) Kanno, T.: Materials for Springs and Their Properties. 1st ed. Tokyo, Nikkan Kogyo Shimbun, 2000, p.136
3) JIS G 4314: Stainless Steel Wires for Springs
4) Kanno, T.: Materials for Springs and Their Properties. 1st ed. Tokyo, Nikkan Kogyo Shimbun, 2000, p.2
5) Yukawa, N. et al.: J. Jpn. Inst. Met. Mater. 31 (7), 851 (1967)
6) JSMA SD010 Compression Coil Spring Heat Resistance Test Method
7) Kato, M. et al.: Material Mechanics. 1st ed. Tokyo, Asakura Publishing, 2009, p.44
8) Yamasaki, S., Takano, K.: Proceedings of JSSE Conference on Springs and Restitution Effect Nov. 2015, Aichi, 2015-6
9) Research Committee on Springs for Stainless steel: Transactions of JSSE. 14, 75 (1969)
10) Nohara, K., Ono, Y., Ohashi, N.: Tetsu-to-Hagané. 63 (5), 212 (1977)
11) Izumida, H. et al.: SEI Technical Review. (166), 19 (2005)
12) Research Committee on High-Temperature Spring Set of Compression Coil Springs: Transactions of JSSE. 63, 71 (2018)
13) Ungar, T. et al.: Appl. Phys. Lett. 69, 3173 (1999)
14) Akama, A. et al.: ISIJ International. 56 (9), 1675 (2016)
15) Yamasaki, S., Takano, T.: THERMEC'2020, International Conference on Processing & Manufacturing of Advanced Materials, Austria, 2020
16) Takano, K., Fukaya, M., Fukuma, H.: Tetsu-to-Hagané. 85 (3), 229 (1999)
17) Yamasaki, S., Takano, T.: THERMEC'2016, International Conference on Processing & Manufacturing of Advanced Materials, Austria, 2016
18) Yamasaki, S., Takano, K.: CAMP-ISIJ. 27, 907 (2014)
19) Honda, T, Akama, D., Tsuchiyama, T., Takagi, S.: CAMP-ISIJ. 29, 816 (2016)
20) Kissinger, H.E.: Anal. Chem. 29, 1702 (1957)
21) Waseda, Y.: Metal Data Book. 4th ed. Tokyo, Maruzen, 2004, p.22
22) Hasegawa, M.: Stainless Steel Handbook. 3rd ed. Tokyo, Nikkan Kogyo Shimbun, 1995, p.158
23) Narutomi, K., Masumura, T., Tsuchiyama, T., Miyamoto, G., Yamasaki, S.: CAMP-ISIJ. 32 (9), 705 (2019)
24) Ojima, O. et al.: Scripta Materialia. 59, 313 (2008)
25) Hosoi, Y.: Science and Latest Technology of Stainless Steels. 1st ed. Tokyo, Japan Stainless Steel Association, 2011, p.385
26) Yamasaki, S., Takano, K.: Proceedings of JSSE Conference on Springs and Restitution Effect Nov. 2016, Tokyo, 2016-6
27) Yamasaki, S., Takano, K: CAMP-ISIJ. 31 (9), 850 (2018)
28) Enokida, H., Ishihara, M., Yamasaki, S., Takano, K.: Proceedings of JSSE Conference on Springs and Restitution Effect Nov. 2019, Tokyo, 2019-6, p.9


Shota YAMASAKI
Senior Researcher
Plate, Bar & Wire Rod Research & Development Div.
Research & Development Center
Nippon Steel Stainless Steel Corporation
3434 Ooaza-shimata, Hikari City, Yamaguchi Pref.
743-8550


Kohji TAKANO
Director, Doctor of engineering
Plate, Bar & Wire Rod Research & Development Div.
Research & Development Center
Nippon Steel Stainless Steel Corporation


Masayuki TOHJO
Manager
Bar & Wire Rod Product Development Gr
Products Development Div.
Nippon Steel Stainless Steel Corporation


Hiroki SAKAI
Senior Manager
Bar & Wire Rod Product Development Gr
Products Development Div.
Nippon Steel Stainless Steel Corporation


Masayuki TENDO
Senior Manager, Doctor of engineering
Bar & Wire Rod Product Development Gr
Products Development Div.
Nippon Steel Stainless Steel Corporation


Toshihiro ISHIKAWA
Manager
Bar & Wire Rod Management Office
Production Management Department
Hikari Area Yamaguchi Works, Production Division
Nippon Steel Stainless Steel Corporation